STEWARTSON LAYER INSTABILITIES IN A CYLINDRICAL CONTAINER WITH A ROTATING LID

Fotis Sotiropoulos, Yiannis Ventikos, and Donald R. Webster
School of Civil and Environmental Engineering
Georgia Institute of Technology
Atlanta, GA 30332-0355
USA

ABSTRACT

Unsteady, three-dimensional computations and flow visualization experiments are carried out to study the onset of instabilities along the sidewall of a closed cylindrical container with a rotating lid. The computations simulate the impulsive spin-up from Re=3000 to Re=6000 for a cylinder of height-to-radius aspect ratio equal to 1.75. During the early stages of the spin-up, travelling Taylor-like ring vortices are shed from the rotating lid. The rings are initially axisymmetric but become azimuthally wavy as they approach the stationary cover. The appearance of the ring-mode is followed by the emergence of four pairs of quasi-stationary spiral vortices, which spread across the cylinder wall and cause the sidewall boundary layer to detach along spiral separation lines. Such lines are also detected in the laboratory flow visualization using aluminum paint pigment flakes. Visualization experiments are also carried out for Reynolds numbers higher than those simulated to further elucidate the evolution of the spiral mode and explore the onset of secondary instabilities.

INTRODUCTION

Rotating flows in cylindrical containers have been and continue to be the subject of intense research. Laboratory models using such configurations have often been employed to study wind-driven ocean circulations (Pratte and Hart, 1991), instabilities of side-wall layers (Hart and Kittleman, 1996; etc.), fundamental aspects of astrophysical flows (Read and Hide, 1983), and the breakdown of coherent vortices (Escudier, 1984). In spite of numerous important contributions, there are still several aspects of rotating flows that are not entirely understood. Most previous work has focused primarily on flow visualization experiments, which, given the complexities of such flows, can only provide limited information. Although some computational investigations have been reported as well, they have all employed axisymmetric equations (Lopez 1998) and, thus, could not elucidate three-dimensional instabilities observed in experiments. In this work we report both unsteady, three-dimensional computations and visualization experiments for a specific sub-class of rotating flows, that generated in a closed cylindrical container by a rotating endwall (figure 1). For brevity, we shall refer to this flow as the container problem.

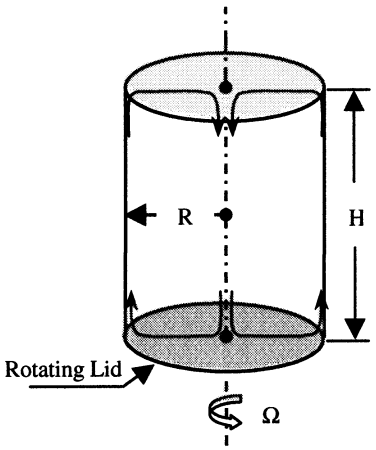

Figure 1. Schematic of the cylindrical container configuration ($Re=\Omega R^2/\nu$)

The container problem has long been used as a test-bed for studying fundamental aspects of the axisymmetric, so-called bubble-type, form of vortex breakdown (Escudier 1984). In a recent experiment, however, Spohn et al. (1998) showed that the vortex breakdown bubbles in this geometry exhibit distinct asymmetric features, which become very pronounced and clearly visible when viewed at the scale of the bubble and with the proper visualization techniques. They attributed these near-axis asymmetries to the existence of "asymmetric flow separations" (Spohn et al. 1998) inside the cylindrical wall boundary layer. In two recent three-dimensional computational studies, Sotiropoulos and Ventikos (1998, 1999) reproduced these three-dimensional features of the container flow and explained their underlying physics. They showed that the container flow is dominated by the centrifugal instability of the sidewall Stewartson layer, which manifests itself in the form of four pairs of counter-rotating spiral vortices. The interaction of the three-dimensional sidewall layer with the stationary cover leads to the asymmetric flow separations observed by Spohn et al. (1998). Sotiropoulos and Ventikos (1999) also elucidated the details

of the flow in the interior of the breakdown bubbles and explained the origin of its asymmetric features.

In this paper, we build upon our previous work in order to further clarify the three-dimensional characteristics of the side-wall layer in the container flow at Reynolds numbers higher than those already studied. A significant novelty of this contribution is the integration, for the first time for such flows, of both visualization experiments and direct numerical simulations. Our results shed new light into the various instability modes of Stewartson layers; underscore the difficulties in conducting meaningful flow visualization experiments; and demonstrate the need for a combined numerical and experimental research strategy for further progress.

DESCRIPTION OF THE NUMERICAL METHOD

The numerical method is second-order accurate both in space and time. It solves the unsteady, three-dimensional, incompressible Navier-Stokes equations using a finite-volume, dual time-stepping artificial compressibility approach. A detailed description can be found in Sotiropoulos and Ventikos (1998).

The subsequently presented results have been obtained on a computational mesh consisting of 153x97x97 grid nodes, in the axial and transverse directions respectively. The curvilinear mesh topology used in Sotiropoulos and Ventikos (1998, 1999) is also employed herein as it acts to naturally excite the sidewall instability modes without requiring ad-hoc numerical triggering techniques. The uniqueness and grid-topology-independence of the computed solutions has been established in Sotiropoulos and Ventikos (1999).

A container with aspect ratio H/R = 1.75 is simulated, which is similar to that employed in the experiments of Spohn et al. (1998). Starting from the steady state solution for Re=1,850 (see Sotiropoulos and Ventikos (1999) for a discussion of the flowfield at this Reynolds number), we impulsively spin up the rotating lid twice, first to Re=3,000 and then to Re=6,000. The computation at Re=3,000 is continued until the flow along the cylindrical sidewall reaches a quasi-steady equilibrium state characterized by the presence of quasi-stationary spiral vortical structures (see figure 2a). The establishment of such a state is consistent with the experimental findings of Spohn et al. (1998) who also found the side-wall flow to be stable in time, even at Reynolds numbers well above the critical level for the onset of oscillatory flow in the interior of the container (for more details see Sotiropoulos and Ventikos 1999). Due to space limitations we only present results for the high Reynolds number case (Re=6,000).

DESCRIPTION OF THE EXPERIMENTS

The visualization experiments were performed in a rigid acrylic cylinder with inner diameter of 203 mm. The height of the motionless upper end wall of the test cell was fixed at H/R = 1.75. The lower end wall rotated at speeds up to 140 rpm, driven by a variable-speed DC motor. The gap between the rotating disk and the cylinder wall was less than 0.3 mm. The disk surface rotated smoothly with variation less than 0.025 mm. The near-wall flow was extremely sensitive to perturbations arising from irregularities in the gap and the disk flatness. In particular, variations in the gap dimension led to the continuous shedding of axisymmetric vortex rings (similar to Taylor vortices) even for Reynolds numbers in the steady flow regime. These apparatus-induced rings overwhelm and mask the three-dimensional instability, thus making the flow visualization a great challenge.

The working fluid was a water and glycerin mixture (roughly 56% glycerin by weight). At a temperature of 24.4°C, the fluid had a specific gravity of 1.136 and a viscosity of 6.95 cP. The cylinder was mounted in a square tank (305 mm per side) filled with the working fluid to a level slightly higher than the top of the test cell. The temperature of the reservoir fluid was monitored continuously and did not vary more than a few tenths of a Centigrade over several hours of experiments.

For the flow visualization, aluminum paint pigment flakes were suspended in the flow. The flakes align themselves with the stream surfaces (Savaş, 1985), and reveal the three-dimensional spiral vortices observed in the computations. The flow is illuminated from above using fluorescent bulbs and the images were captured with a 1Kx1K digital camera.

RESULTS AND DISCUSSION

To elucidate the complex three-dimensional structure of the sidewall boundary layer, we examine the numerical solutions in terms of: i) instantaneous iso-surfaces of radial velocity component; ii) limiting streamlines along the cylinder wall; and iii) three-dimensional particle trajectories. In this cylindrical geometry, radial velocity iso-surfaces of opposite sign can effectively visualize vortical structures along the cylinder wall. Limiting streamlines and particle paths, on the other hand, provide images that can be compared with laboratory visualizations. It is important to emphasize that the simulations were still under way during the preparation of this manuscript, and, thus, the subsequent computed results focus on the early stages of the impulsive spin-up from Re=3000 to 6000 (the simulated interval corresponds to approximately 10 lid revolutions). A comprehensive discussion of the temporal evolution of the flow at later times will be included in a future publication. We should also point out that since the main objective of this paper is to study the instabilities of the Stewartson layer, the very complex flowfield in the interior of the container will not be discussed.

The temporal evolution of the iso-surfaces of radial velocity is shown in figure 2. The initial flowfield (T=0) is an instantaneous solution for Re=3,000. Within approximately one half lid revolution from the impulsive spin-up from Re=3000 to 6000, an upward traveling pair of counter-rotating (see discussion of figure 3 below) ring vortices is shed from the rotating endwall. The initially axisymmetric rings interact with and eventually disorganize the pre-existing spiral vortical structures (see figures 2b and c). This interaction with the three-dimensional sidewall boundary layer causes the rings to become azimuthally wavy as they approach the stationary cover. We should point out that the shedding of the start-up rings is essentially identical to that described by Sotiropoulos and Ventikos (1998) who simulated a similar spin-up process, albeit at considerably

lower Reynolds numbers (from Re=2100 to 3750) and for a somewhat longer container (H/R=2.). An important difference between our earlier work and the present findings is that in Sotiropoulos and Ventikos (1998) the shedding of two ring vortices was immediately followed by the growth of spiral vortices. In the present simulations, however, a second pair is shed from the rotating lid and starts travelling upward (see figure 2c) prior to the emergence of the spiral mode.

The mechanisms that lead to the emergence of this second pair should be related to the step change in Reynolds number (ΔRe=3000), which is the largest among all spin-up numerical experiments we have carried out so far. As discussed in Sotiropoulos and Ventikos (1998), shortly after the start of the impulsive spin-up the centrifugally unstable near-wall layer just above the rotating lid senses the instantaneous increase in azimuthal velocity and momentarily behaves as a "one-dimensional" flow over a concave wall. As the axial velocity inside the Stewartson layer begins to increase, due to Ekman pumping from the container axis toward the periphery, the flow tends to become more two-dimensional and the spiral mode emerges. One could argue, therefore, that for large spin-up increments it would take longer for a sufficiently large axial flow component to build up along the cylinder wall, thus, leading to a temporary preference toward the ring mode. Such argument is consistent with earlier observations by Weidman (1976) who studied experimentally the instability of the Stewartson layer that forms along the side-wall of a cylindrical container initially at solid-body rotation during spin-down. Gradual spin-down led to spiral vortices, while impulsive spin-down caused ring vortices to form.

The rapid disorganization and temporary destruction of the initial spiral vortices by the ring modes, evident in figures 2b to 2d, is particularly illuminating, insofar as the experiments are concerned, and deserves some discussion. As already mentioned above, laboratory visualizations of the spiral vortices were complicated considerably by the continuous shedding of ring vortices from the rotating lid. This phenomenon, which was encountered even at Reynolds numbers for which the flow should have been steady, was found to be the result of apparatus-related disturbances induced by very small imperfections of the experimental rig (disk alignment and wobbling, imperfections in the machining of the cylinder, etc.). These disturbances resulted in a continuous forcing of the flow and gave rise to a sequence of travelling ring vortices which altered the structure of the Stewartson layer and made it impossible to visualize the spiral vortices. Our computed results in figure 2 demonstrate clearly the dramatic impact of the ring mode on the spirals and explain why continuous shedding of ring vortices can mask completely the onset of spiral vortices. The flow visualization photographs discussed below were obtained after carefully minimizing apparatus-induced disturbances.

After approximately three revolutions of the rotating lid (see figure 2e), the spiral vortices re-emerge and spread along the cylinder wall. The final image in the sequence of figure 2 depicts the structure of these vortices after 10 lid rotations. As seen, the spirals have reached the stationary cover and their interaction with the upper corner region has triggered a very complex, and highly three-dimensional flow.

Figure 3 shows the manifestation of the ring and spiral modes in the instantaneous near-wall (limiting) streamlines. Due to space limitations only two instants in time are shown. Figure 3a corresponds to the radial iso-surfaces shown in figure 2c. The two horizontal dark clusterings mark regions where the near-wall flow converges axially and is injected away from the wall to satisfy continuity. When viewed in tandem with the radial iso-surface plots, these lines reveal the presence of two pairs of counter-rotating, azimuthally wavy, ring vortices. The interaction of the rings with the initial spirals is also evident in this plot, as the remnants of the latter are clearly visible near the top cover. Figure 3b shows the near-wall streamlines after the spiral mode has been established (see figure 2f). As seen in this figure, the growth of the spiral vortices causes the boundary layer to separate along four spiral lines of convergence, which consistently form in regions where dark-colored streaks meet the stationary endwall. These streaks mark regions where near-wall fluid is injected toward the center of the container due to the upwash motion between two counter-rotating vortices. Therefore, as the endwall is approached the spiral-vortex-induced radially inward motion within these streaks is further enhanced by the action of the radial pressure gradient, also directed toward the center, causing the flow to separate before reaching the endwall. Fluid particles within the lightly-colored streaks, on the other hand, experience the upwash effect of adjacent vortex pairs that allows them to resist the radial pressure gradient and move closer to the endwall before they separate.

The flow visualization photographs of Spohn et al. (1998) reveal spiral separation lines in the limiting streamlines along the cylinder wall, which are very similar to those shown in figure 3b. Spohn et al. (1998), however, did not link the near-wall streaks with coherent spiral vortices inside the Stewartson layer. Moreover, their photographs, which were obtained by illuminating (with a vertical laser sheet) only a portion of the cylinder wall, can not establish conclusively the total number of spiral separation lines along the circumference. The present experiments were undertaken in order to clarify these issues and provide additional experimental verification of our computational findings. Flow visualization images at three Reynolds numbers, 5,800, 14,000, and 24,000, are shown in figures 4 and 5--figure 4 also includes computed streaklines for comparison. In each case, the flakes highlight the structure of the instability waves along the cylinder wall.

Our experimental results re-enforce and further clarify the findings of Spohn et al. (1998). Figure 4a shows clearly a single spiral line along the cylinder wall. In accordance with Spohn et al. (1998), we too observed this line to remain stable in time even though the flow for Re=6000 is within the unsteady regime. The fact that only one spiral is present in the photograph appears to be in contrast with the n=4 spiral mode we found in the computations. To explore this issue, we calculate the trajectories of 200 markers, initially distributed along a circle just off the cylinder wall, within the instantaneous flowfield shown in figures 2f and 3b (T=31.9). Although the resulting image (figure 4b) does not correspond to true streaklines (since the flow is unsteady), it should be

much closer, than the two-dimensional limiting streamlines in figure 2, to what we actually observe in the laboratory. As seen in figure 4b, when the computed flowfield is visualized in that manner one well defined spiral line (oriented from right to left) emerges on the front face of the cylinder--the left-to-right spiral that is also visible in this figure is located at the diametrically opposite side of the container. The computed and observed spirals are inclined at the same angle but the former appears to be located somewhat closer to the rotating lid than the latter. This discrepancy, however, could be to the fact that our simulations have not progressed sufficiently in time for the Stewartson layer flow to approach the quasi-steady equilibrium that has been established in the experiment. It is important to point out that the number of spiral lines that are visible in the numerical visualization was found to be highly depended on the azimuthal orientation of the cylinder. That is, rotating figure 4b around its vertical axis can lead to views with two or even three spiral lines. This finding demonstrates the enormous difficulties in interpreting laboratory visualizations of complex three-dimensional flows and underscores the fact that experiments and numerical simulations must proceed synergistically.

As shown in figure 5, when the Reynolds number is increased the instability of the side-wall layer intensifies and becomes easier to visualize. Three spiral lines are clearly visible for Re=14,000 and Re=24,000. For the latter case the spirals are distorted by what appears to be another set of spiral waves, oriented from left to right. This new instability mode could be similar to that detected by Hart and Kittelman (1996) in a related Stewartson layer flow. Hart and Kittelman (1996) attributed the emergence of this new set of spiral waves in their experiment to the growth of a transverse shear instability mode. We have also reproduced computationally (Sotiropoulos and Ventikos 1999) this new set of spiral waves in a somewhat longer container. Our visualization photograph, however, lacks the necessary clarity to draw definitive conclusions. Additional experiments are currently underway to further explore this aspect of the flow.

CONCLUSIONS

Flow visualization experiments and direct numerical simulations have been conducted to elucidate the structure of the Stewartson layer in a closed cylindrical container with a rotating lid. The numerical simulations show that shortly after the impulsive spin-up form Re=3000 to 6000, travelling pairs of counter-rotating ring vortices are shed above the rotating lid. These rings are initially axisymmetric but become azimuthally wavy as they approach the stationary cover. The onset of the ring mode is followed by the emergence of four pairs of counter-rotating spiral vortices. The upwash effect of these vortices causes the side-wall boundary layer to detach along four spiral separation lines. Laboratory visualizations, using aluminum paint pigment flakes, capture the onset of the spiral mode along the cylinder wall and provide new evidence that support and further clarify the recent findings of Spohn et al. (1998). Our work demonstrates the enormous challenges that unstable, rotating flows pose to visualization techniques and underscore the need for combined numerical and experimental investigations.

Currently, we are continuing the calculations to obtain a time history sufficiently long for conducting a comprehensive quantitative analysis of the flowfield. Additional calculations will also be carried out at higher Reynolds numbers to explore the evolution of the spiral vortices, the growth of the secondary instabilities, and ultimately the mechanisms that lead to transition to turbulence. These calculations will be supplemented by more detailed qualitative and quantitative experiments.

ACKNOWLEDGMENTS

All calculations were carried out on the Cray T-90 supercomputer at the San Diego Supercomputer Center. Thanks to Todd Taylor for assisting with the flow visualization experiments.

REFERENCES

Escudier, M. P. (1984), "Observations of the flow produced in a cylindrical container by a rotating endwall," *Exp. Fluids* 2 4, pp. 189-196.

Hart, J. E., and Kittelman, S. (1996), "Instabilities of the Sidewall Boundary Layer in a Differentially Driven Rotating Cylinder," Phys. Fluids 8 (3), pp. 692-696

Lopez, J. M. (1996), "Stability of Stationary Endwall Boundary Layers During Spin-Down," *J. Fluid Mech.* 326, pp. 373-398.

Pratte, J. M., and Hart, J. E. (1991), "Experiments on Periodically Forced Flow over Topography in a Rotating Fluid," *J. Fluid Mech.* 77, pp. 153-175.

Read, P. L. and Hide, R. (1983), "Long-Lived Eddies in the Laboratory and in the Atmosphere of Jupiter and Saturn," *Nature* 302, 126.

Savaş, Ö., "On flow visualization using reflective flakes," *J. Fluid Mech.*, vol. 152, pp. 235-248 (1985).

Sotiropoulos, F., and Ventikos, Y. (1999), "The Three-Dimensional Structure of Confined Swirling Flows with Vortex Breakdown," under review in the *J. Fluid Mech.*

Sotiropoulos, F., and Ventikos, Y. (1998) "Transition from Bubble Vortex Breakdown to a Columnar Vortex in a Closed Cylinder with a Rotating Lid," *Int. J. Heat Fluid Flow* 19, 446-458.

Spohn, A., Mory, M., and Hopfinger, E.J. (1998), "Experiments on vortex breakdown in a confined flow generated by a rotating disk," *J. Fluid Mech.* 370, pp. 73-99.

Weidman, P. D. (1976), "On the Spin-Up and Spin-Down of a Rotating Fluid. Part 2. Measurements and Stability," *J. Fluid Mech.* 77(4), pp. 709-735.

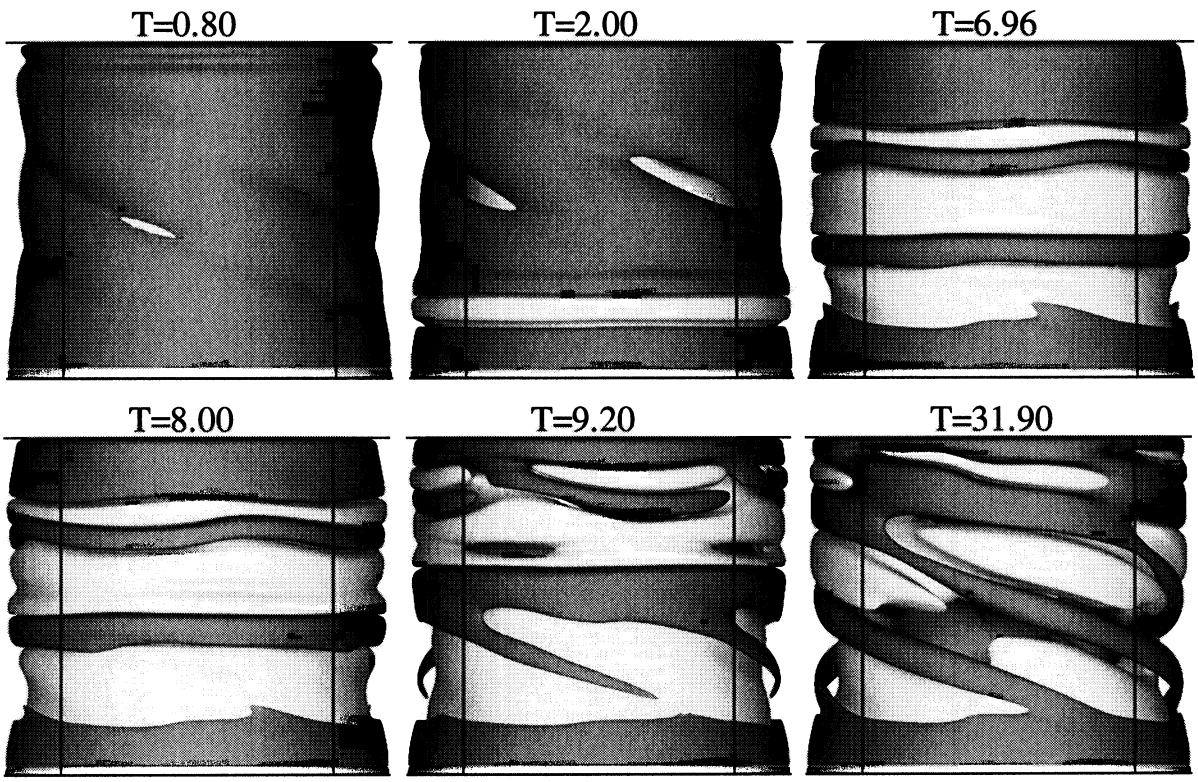

Figure 2. Iso-surfaces of constant radial velocity component showing the growth of roll and spiral modes inside the Stewartson layer during impulsive spin-up from Re=3000 to Re=6000. Dark and light surfaces correspond to U_r=-0.003 and 0.001 respectively. Time is measured from the start of the impulsive acceleration (the rotating lid completes one revolution in π time units).

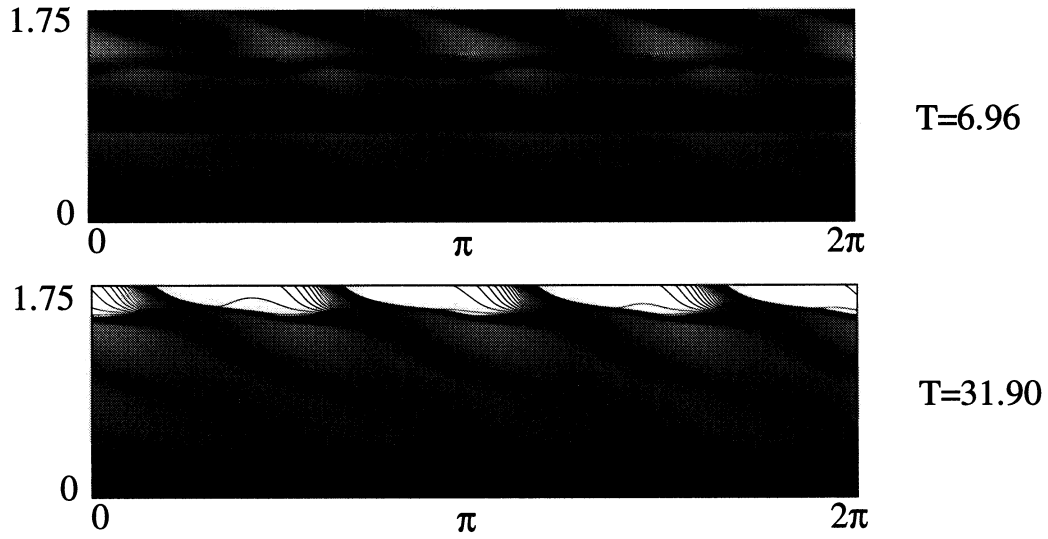

Figure 3. Instantaneous limiting streamlines along the cylinder wall during impulsive spin-up. Streamlines are shown on a cylindrical surface located at r=0.99R. The surface has been unfolded and plotted as a rectangle in terms of the axial and circumferential coordinates.

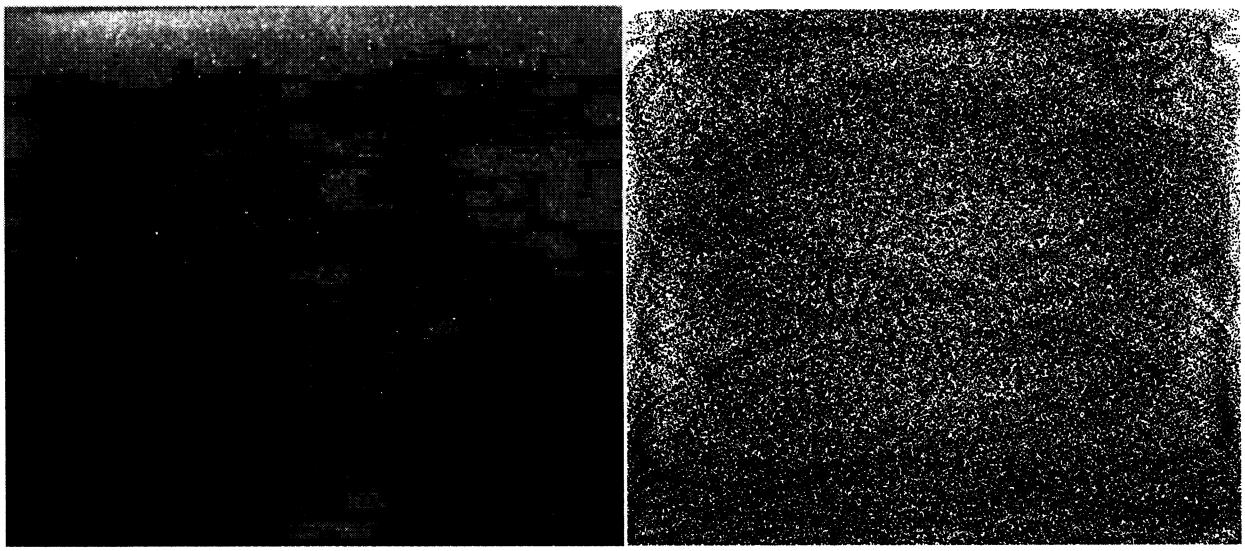

(a) (b)

Figure 4. a) Experimental visualization of the side-wall flow using aluminum paint pigment flakes (Re=5,800)
b) Calculated instantaneous streaklines for the flowfield shown in figure 2f (Re=6,000)

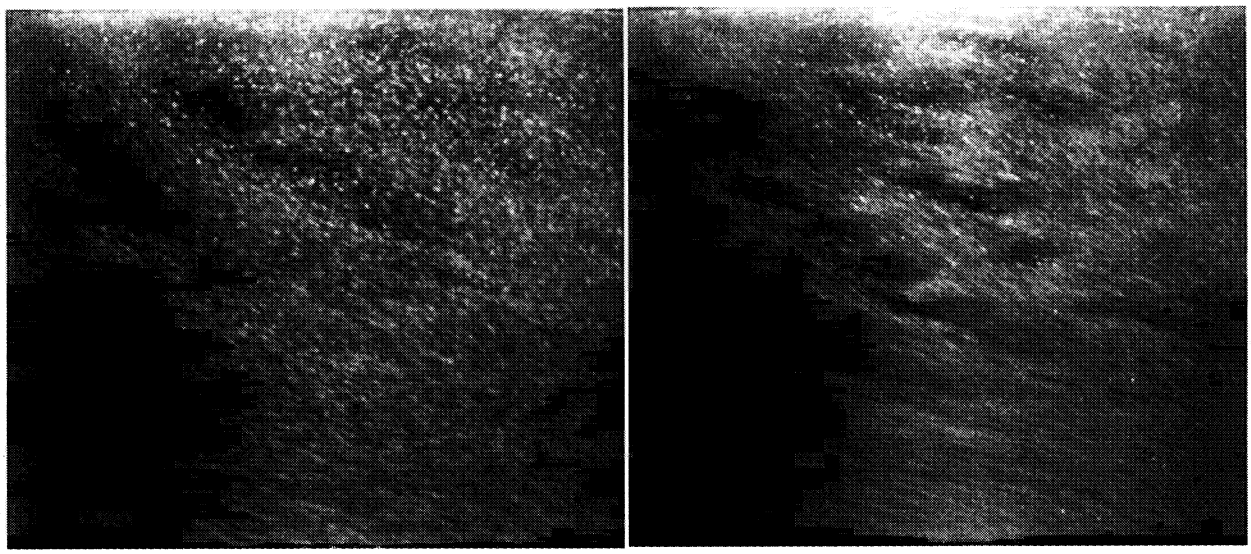

(a) (b)

Figure 5. Experimental visualization of the side-wall flow using aluminum paint pigment flakes
a) Re=14,000; b) Re=24,000